

# Active Power Filter Implementation Using a Four Leg VSI for Renewable Power Generation Systems

Sai Satya Mounisha Thurumalla<sup>1</sup>, V Sushma Munagapati<sup>2</sup>, Neeraja Modempudi<sup>3</sup>, Venkatesh Amara<sup>4</sup>, E. Rambabu<sup>5</sup>

<sup>1,2,3,4</sup>Department of Electrical Engineering, Sree Venkateswara College of Engineering, North Rajupalem, Nellore, Andhra Pradesh, India

<sup>5</sup>Guide, Assistant Professor, M.Tech, Department of Electrical Engineering, Sree Venkateswara College of Engineering, North Rajupalem, Nellore, Andhra Pradesh, India

**Abstract:** Renewable generation affects power quality due to its nonlinearity, since solar generation plants and wind power generators must be connected to the grid through high-power static PWM converters. The harmonics produced by the non-linear loads at the point of common coupling deteriorate the power quality. The effective method to mitigate the harmonics is the implementation of the active power filter with a four-leg voltage-source inverter using a predictive control scheme. Traditionally, active power filters have been controlled using pre-tuned controllers such as PI- type or adaptive, for the control of current as well as the dc voltage loops which are based on the equivalent linear model. An active power filter implemented with the four-leg VSI using a novel predictive scheme is presented in this paper. Under steady state and transient operating conditions the compensation performance of the active power filter is demonstrated using MATLAB/SIMULINK. The results show the predictive method controls very effectively the load and performs very well compared with that of the classical solutions.

**Keywords:** Shunt active power filter, PWM converters, SRF-PLL, Predictive control algorithm, 4-leg VSI.

## 1. Introduction

Electric utilities and end users of electric power are becoming increasingly concerned about meeting the growing energy demand. But increasing air pollution global warming concerns, diminishing fossil fuels it made necessary to look towards the renewable sources as future energy solution. The renewable power generation systems may pose a threat to the network in terms of stability, voltage regulation and power quality issues. With the advancement in power electronics and digital control technology, the RES systems can be actively controlled to enhance the system operation with improved PQ and PCC.

Generally, current control voltage source inverters are used to interface the intermittent RES in distributed system. But the exact calculation of network inductance in real-time is difficult and may deteriorate the control performance. The non-linear load current harmonics may result in voltage harmonics and can create a serious PQ problem in the power system network. Active power filters are extensively used to compensate the load current harmonics and load unbalance at distribution level. In this paper mathematical model of 4-leg VSI and the principles of operation of the proposed predictive control scheme is presented. Predictive model which is a non linear- model is very close to real operating conditions. The controller under the transient operating conditions improves the performance of the active power filter because it can follow the current reference signal quickly by maintaining a constant dc-voltage. The grid-interface inverter can effectively be utilized to perform following important functions: 1) transfer of active power harvested from the renewable resources; 2) load reactive power demand support; 3) current harmonics compensation at PCC and 4) current unbalance and neutral current compensation in case of 3-phase 4-wire system. The predictive control is a intuitive control scheme that handles multivariable

characteristics, simplifies the treatment of dead time compensations in case of motor drive applications.

## 2. System Description

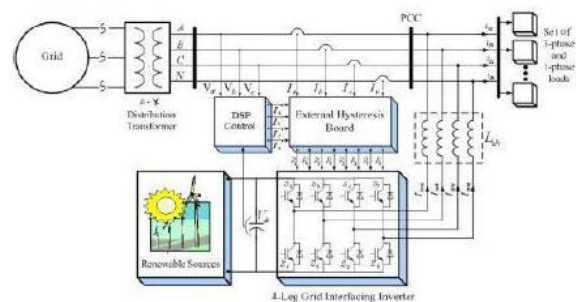


**Figure 1:** Schematic diagram of proposed renewable based distributed generation system.

The proposed system consists of renewable sources used to generate electricity for residential and small industries used dc/ac and ac/ac static PWM converters for voltage conversion and static PWM converters for voltage conversion and battery banks. The maximum power point tracking performed by converters, extract the maximum energy possible from wind and sun. The dc-capacitor decouples the RES system from grid and also allows independent control of converters on either side of the dc-link.

## 3. Modelling and Control

As shown in Figure 2 the rectifier is a three- phase fully-controlled bridge consisting of six power transistors connected to three- phase power source by means of a filter. The later is given by inductance and the parasitic resistance. The neutral point is electrically floating.

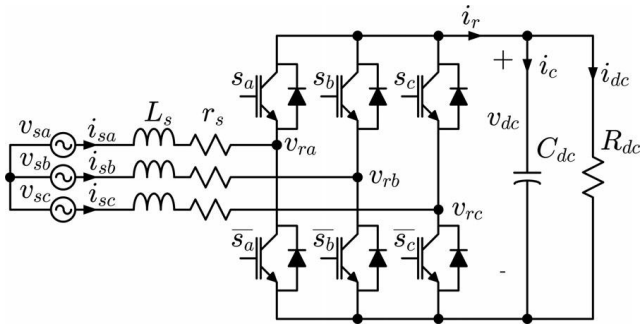


Figure 2: AFE rectifier with floating neutral point

The converter topology is similar to the conventional three-phase converter with fourth leg connected to the neutral bus of the system. The fourth leg increases the switching states from 8 to 16, improving control flexibility and output voltage quality. The voltage in any leg  $x$  of the converter, measured from the neutral point ( $n$ ), can be expressed in terms of switching states, as follows:

$$v_{un} = S_u - S_n v_{dc} \tag{1}$$

The mathematical model of the filter derived from the equivalent circuit as shown in figure 2

$$v_0 = v_{un} - R_{eq} i_0 - L_{eq} \frac{di_0}{dt} \tag{2}$$

Where  $R_{eq}$  and  $L_{eq}$  are the 4L-VSI output parameters expressed as Thevenin impedances at the converter output terminals ( $Z_{eq}$ ). Therefore, the Thevenin equivalent impedance is determined by a series connection of the ripple filter impedance and a parallel arrangement between the system equivalent impedance  $Z_s$  and the load impedance  $Z_L$ .

$$Z_{eq} = \frac{Z_s Z_L}{Z_s + Z_L} + Z_f \approx Z_s + Z_f. \tag{3}$$

For this model, it is assumed that  $Z_s \gg Z_L$ , that the resistive part of the system's equivalent impedance is neglected, and the series reactance in the range of 3-7% p.u., which is an acceptable approximation of the real system. Finally in Eq(2)  $R_{eq} = R_f$  and  $L_{eq} = L_f + L_s$ .

#### 4. Digital Predictive Current Control

This control scheme is basically an optimization algorithm which is to be developed using discrete mathematics in order to consider additional restrictions such as time delays and approximations. The proposed predictive control strategy is based on the fact that only a finite number of possible states of switches can be generated by static power converter and the models of the system can be used to predict the behavior of the variables for each state of switching. The selected appropriate state of switching can be applied to next interval state. The main characteristic of

the predictive control is the use of the system model to predict the future behavior of the variables to be controlled. This information is given to the controller to select the optimum switching state that will be applied to the power converter according to obtained optimization criteria. This algorithm is easy to implement and understand, and it can be implemented with three main blocks, as shown in Figure 3.

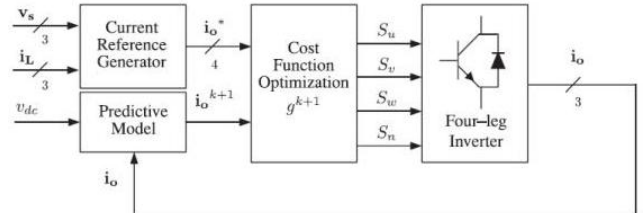


Figure 3: Predictive current control block diagram current reference generator

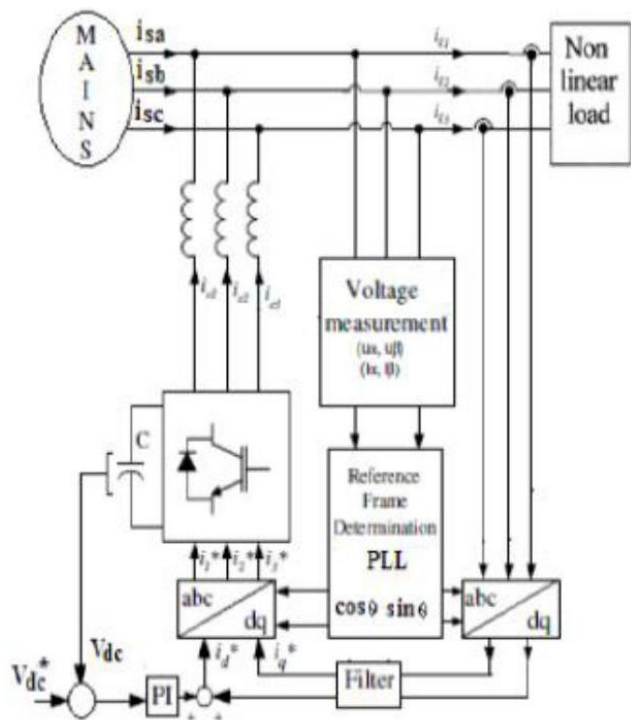
1)Current Reference Generator: This unit is designed to generate the required current reference that is used to compensate the undesirable load current components. The system voltages, the load currents, and the dc-voltage converter are measured, while the neutral output current and the load current are generated directly from these signals.

2)Prediction Model: The converter model is used predict the output converter current. Here the controller operates in discrete time; both the controller and the system model must be represented in a discrete time domain. The discrete time model consists of a recursive matrix equation that represents a predictive system. This means that for a given sampling time  $T_s$ , knowing the converter switching states and control variables at instant  $kT_s$ , it is possible to predict the next states at any instant  $[k + 1] T_s$ . The algorithm calculates all 16 values associated with the possible combinations that the state variables can achieve. This predictive model is used to predict the output converter current.

$$\frac{dx}{dt} \approx \frac{x[k + 1] - x[k]}{T_s}. \tag{4}$$

The 16 possible output current predicted values can be obtained from (2) and (4).

$$i_o[k + 1] = \frac{T_s}{L_{eq}} (v_{xn}[k] - v_o[k]) + \left(1 - \frac{R_{eq} T_s}{L_{eq}}\right) i_o[k]. \tag{5}$$



In the SRF, the load current signals are transformed into conventional rotating frame d-q. If  $\theta$  is the transformation angle, the transformation is defined by

$$\begin{bmatrix} x_d \\ x_q \end{bmatrix} = \sqrt{\frac{2}{3}} \begin{bmatrix} \cos(\theta) & \cos(\theta - \frac{2\pi}{3}) & \cos(\theta - \frac{4\pi}{3}) \\ -\sin(\theta) & \sin(\theta - \frac{2\pi}{3}) & -\sin(\theta - \frac{4\pi}{3}) \end{bmatrix} \begin{bmatrix} x_a \\ x_b \\ x_c \end{bmatrix} \quad (7)$$

Where X denotes voltages or currents.

In the SRF  $\theta$  is a time varying angle that represents the angular position of the reference frame which is rotating at a constant speed in synchronism with the three phase ac voltages. The synchronizing method used to implement SRF is the Phase Locked Loop (PLL). In this case the speed of the reference frame is practically constant, that is, the method behaves as a reference frame's moment of inertia is finite.

As shown in (5), in order to predict the output current  $i_o$  at a instant  $(k + 1)$ , the input voltage value  $v_o$  and the converter output voltage  $v_xN$ , are required.

3) Cost Function Optimization: The cost function optimization is a quality function evaluates the error between reference and predicted currents in the next sampling interval. The voltage which value minimizes the current error in selected and applied to the load.

$$\begin{aligned} g[k + 1] = & (i_{ou}^*[k + 1] - i_{ou}[k + 1])^2 \\ & + (i_{ov}^*[k + 1] - i_{ov}[k + 1])^2 \\ & + (i_{ow}^*[k + 1] - i_{ow}[k + 1])^2 \\ & + (i_{on}^*[k + 1] - i_{on}[k + 1])^2. \end{aligned} \quad (6)$$

The 16 predicted values obtained for  $i_o[k + 1]$  are compared with the reference currents using a cost function. The output current predictive block  $i_o[k + 1]$  is equal to the reference  $i_o^*[k+1]$  when  $g=0$ . Therefore, the optimization goal of the cost function is to achieve a  $g$  value close to zero. During each sampling state, the switching state that generates the minimal value of  $g$  is selected the 16 possible function values.

#### 4.1. Synchronous Reference Frame (SRF)

##### For Current Reference Generator

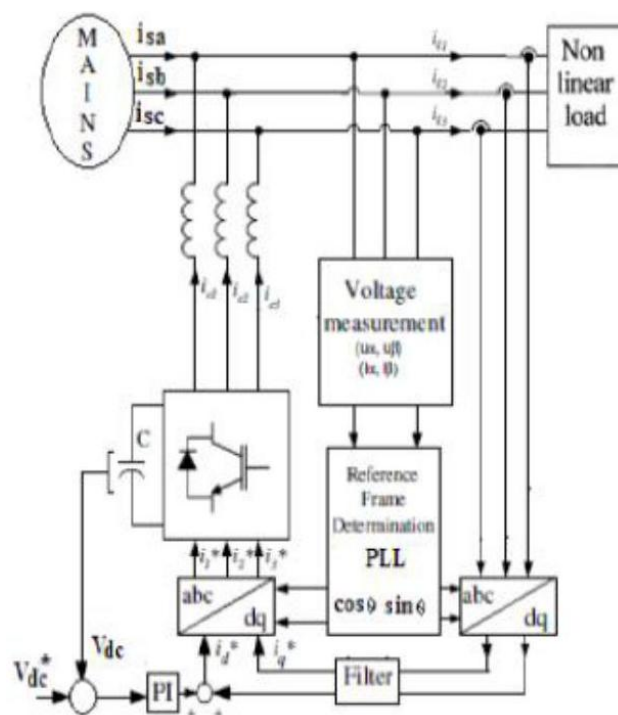


Figure 4: Basic Synchronous Reference Frame Configuration

### 5. dq-Base Current Reference Generator

#### Modelling:

A dq-based current reference generator scheme is used to obtain the active power filter current reference signals. This scheme presents the fast and accurate signal tracking capability. This scheme avoids the voltage fluctuations that deteriorate the current reference signal performance of compensation.

This dq-based scheme operates in a rotating reference frame, hence the measured currents must be multiplied by the  $\sin(\omega t)$  and  $\cos(\omega t)$  signals. By the use of dq transformation, the d current component is synchronized with the corresponding phase to neutral system voltage, the q current component is phase shifted by 90.  $\sin(\omega t)$  and  $\cos(\omega t)$  synchronized reference signals are obtained from a synchronous reference frame (SRF) PLL.

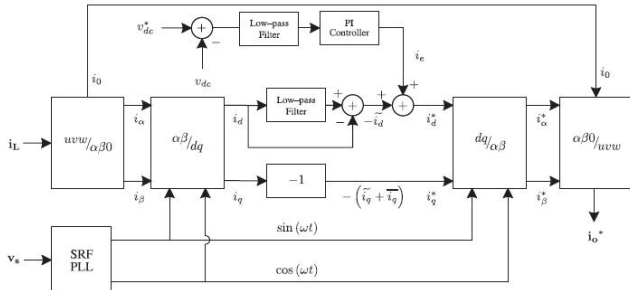


Figure 5. dq based current reference generator block diagram Tracking errors are eliminated, since SRF-PLLs are designed to avoid phase voltage unbalancing, harmonics ( i.e less than 5% and 3% in fifth and seventh harmonics respectively) and off-set caused by the non linear load conditions and measurement errors.

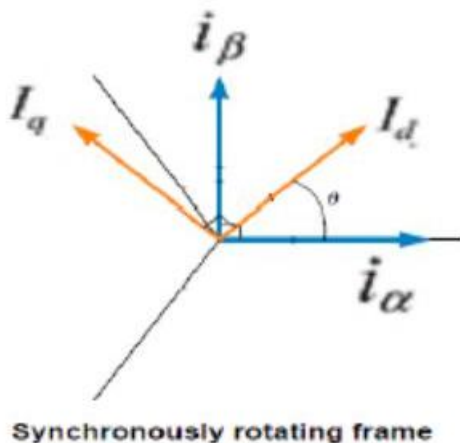
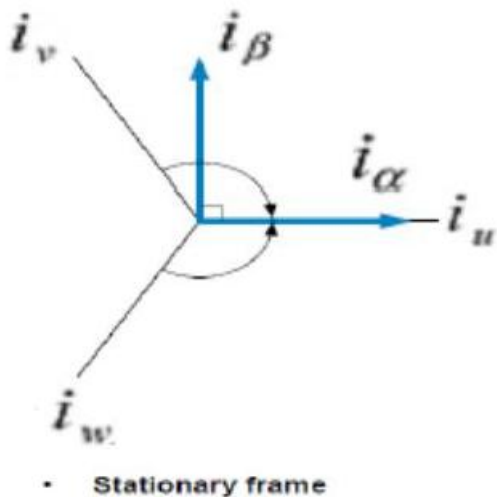


Figure 6: Vector representation of abc to dq transformation

The transformation is done two steps:

- 1)The three-phase stationary transformation of coordinate system to the two-phase so-called  $\alpha\beta$  stationary coordinate system.
- 2)A transformation from the  $\alpha\beta$  stationary coordinate system to the  $\alpha\beta$  rotating coordinate system in Figure 6.
- 3)Figure6. Vector representation of abc to dq transformation to transform the abc to  $\alpha\beta$  using

**Clark transformation**

$$\begin{bmatrix} i_d \\ i_q \end{bmatrix} = \sqrt{\frac{2}{3}} \begin{bmatrix} \sin \omega t & \cos \omega t \\ -\cos \omega t & \sin \omega t \end{bmatrix} \begin{bmatrix} 1 & -\frac{1}{2} & -\frac{1}{2} \\ 0 & \frac{\sqrt{3}}{2} & -\frac{\sqrt{3}}{2} \end{bmatrix} \begin{bmatrix} i_{Lu} \\ i_{Lv} \\ i_{Lw} \end{bmatrix} \quad (8)$$

A low-pass filter (LPF) extracts the dc component of the phase currents  $i_d$  to generate the harmonic reference components  $-id$ . The reactive reference components of the phase- currents are obtained by phase-shifting the corresponding ac and dc components of  $i_q$  by 180. To keep the dc voltage constant the amplitude of the converter reference current must be modified by adding active power reference signal  $i_e$  with the d-component. The resulting signals are transformed back to a three-phase system by applying the Inverse Park and Clark transformation as shown in fig (9). The cut of frequency of the LPF used in the paper is 20 Hz.

$$\begin{bmatrix} i_{ou}^* \\ i_{ov}^* \\ i_{ow}^* \end{bmatrix} = \sqrt{\frac{2}{3}} \begin{bmatrix} \frac{1}{\sqrt{2}} & 1 & 0 \\ \frac{1}{\sqrt{2}} & -\frac{1}{2} & \frac{\sqrt{3}}{2} \\ \frac{1}{\sqrt{2}} & -\frac{1}{2} & -\frac{\sqrt{3}}{2} \end{bmatrix} \times \begin{bmatrix} 1 & 0 & 0 \\ 0 & \sin \omega t & -\cos \omega t \\ 0 & \cos \omega t & \sin \omega t \end{bmatrix} \begin{bmatrix} i_0 \\ i_d^* \\ i_q^* \end{bmatrix} \quad (9)$$

Which is produced cannot be removed and therefore generates a third harmonic in the reference current when it is converted back to abc frame.

**5.1 DC Voltage Control**

The dc voltage remains constant, until the active power absorbed by the converter decreases to level where it is unable to compensate for its losses. The slow dynamic response of the voltage across the electrolytic capacitor does not affect the current transient response. Therefore PI controller represents a simple and effective alternative for dc-voltage control.

The error (e) is processed by a PI controller, with two gains,  $k_p$  and  $k_i$ , both gains are calculated according to the dynamic response requirement.

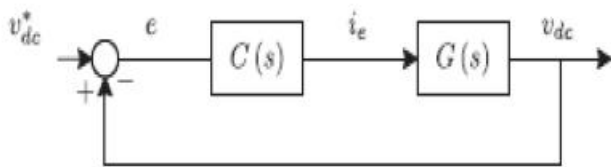


Figure 7: Dc voltage control block diagram

The active power absorbed by the converter is controlled by adjusting active power reference signal. Fig 7 shows the output of the PI controller is fed to the dc-voltage transfer function G(S) which is represented by a first order Equation (10)

$$G(s) = \frac{v_{dc}}{i_e} = \frac{3 K_p v_s \sqrt{2}}{2 C_{dc} v_{dc}^* s} \quad (10)$$

### 6. Flow Chart for Predictive Control

The figure 8 shows the flow chart of the predictive control method. The input values taken as the  $i_0, S[tk]$  predefined values of the compensating current and switching state. Based on these values the predictive control block calculates the  $i_0[k+1]$  value, repeats the process until 16 predictive values. Reference current values calculate from dq- base reference current method and compare those values predictive values which have maximum error value select the particular switching state then apply to VSI. One of the major advantages of this method is that it allows the implementation of a linear controller in the dc-voltage control loop. The disadvantage of this method is that it generates the second order harmonic component under unbalanced operating conditions. The second harmonic of a discrete model that can be easily implemented in real-time interface (RTI). Simulations were performed considering a  $20 [\mu s]$  of sample time.

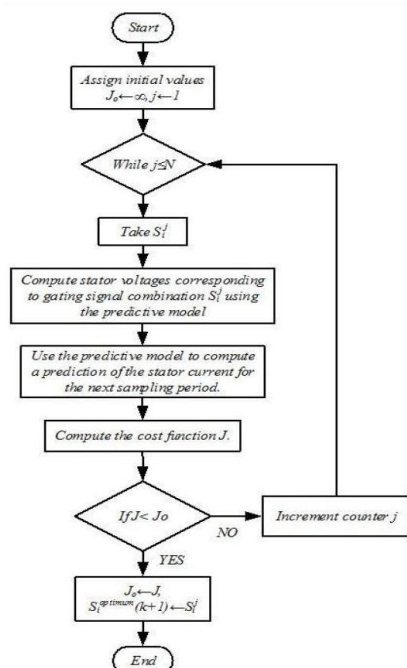


Figure 8: Flow chart for Predictive controller

### 7. Simulation Results

Table 1: Specification of parameters

S. No	Variable	Description	Value
1	$v_s$	Source voltage	55V
2	F	System frequency	50Hz
3	$v_{dc}$	DC voltage	162V
4	$c_{dc}$	DC capacitor	2200 $\mu$ F
5	$L_f$	Filter Inductor	50mH
6	$R_f$	Internal resistance with in $L_f$	0.6 $\Omega$
7	$T_s$	Sampling time	20 $\mu$ s

A simulation model for the three-phase four-leg PWM converter designed using table1 parameters; it has been developed in MATLAB/SIMULINK. The objective is to verify the current harmonic compensation effectiveness of the proposed control scheme under different operating conditions. The proposed predictive control algorithm was programmed using a S-function block that allows simulation.

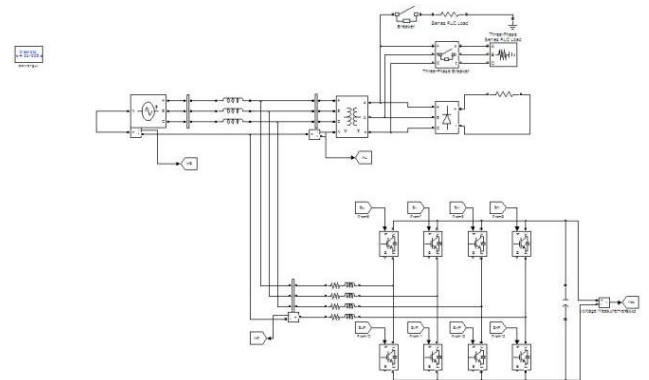


Figure 9: Simulink block diagram

#### Case 1: Single Phase results of proposed Shunt active power filter

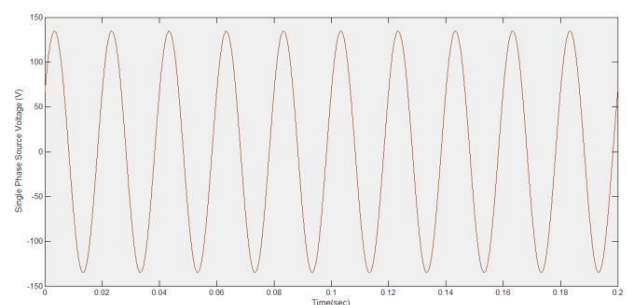


Figure 10 (a): phase to neutral source voltage

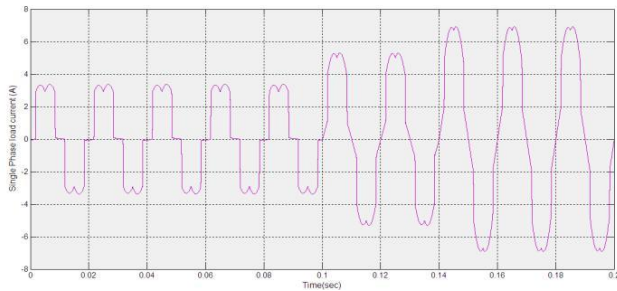


Figure 10 (b): Single phase load current

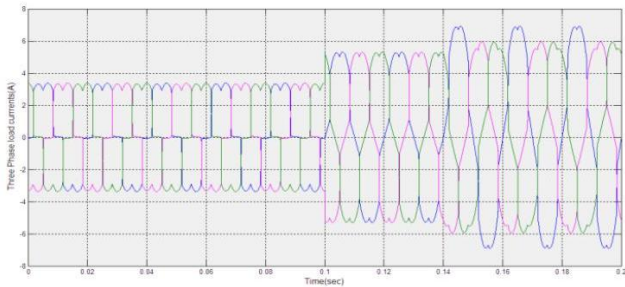


Figure 11 (a): Three phase load currents

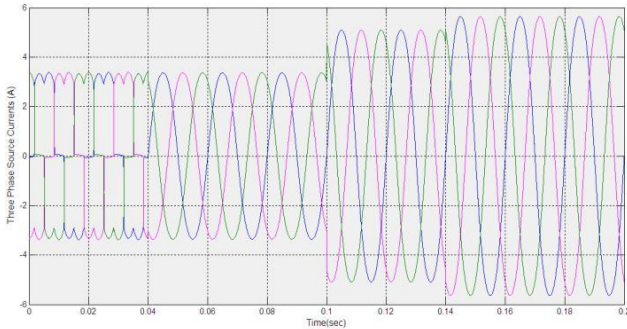


Figure 11 (b): Three Phase Source Currents

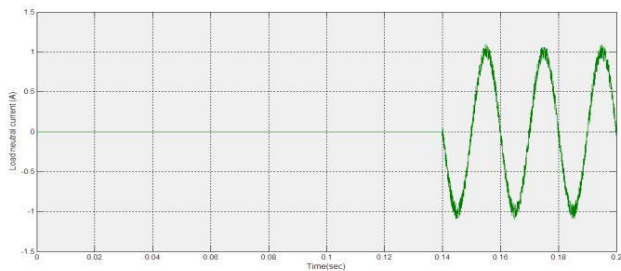


Figure 11(c): Load neutral current

At  $t=0.14\text{sec}$  the single phase unbalance load is applied which is equivalent to 11% current unbalance at that time load side neutral currents presented as shown in figure 11 (c).

### 7.1 Experimental Results

The compensation effectiveness of the active power filter is corroborated in a 2kVA experimental setup. In order to verify the effectiveness of the current harmonic compensation a six-pulse rectifier is selected as a nonlinear load. An unbalanced load is used to validate the performance of the neutral current compensation. Experimental results as shown in fig 12(a) indicate that the

In figure 11 (a) shows the constant u- phases source voltage. Figure 11(b) shows the u-phase non-linear load currents.

### Case 2: Three phase results of proposed shunt active power filter.

Three phase constant load currents u, v and w shown in Figure 11(a) the source currents remain constants shown in Figure 11(b).again at  $t=0.14\text{sec}$  in u-phase single phase unbalanced load is applied the source voltage maintain pure sinusoidal wave.

total harmonic distortion of the line current is reduced from 27.09% to 4.54%. This is the consequence of the good tracking characteristic of the current references as shown in fig 12 (b).

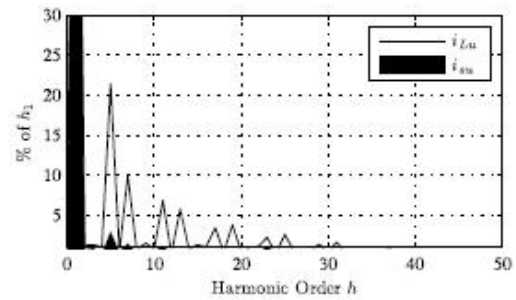


Figure 12(a)

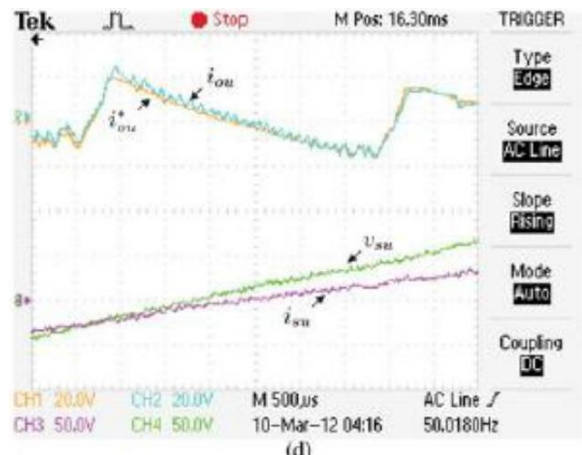


Figure 12(b)

## 8. Conclusion

Improved dynamic current harmonics and a reactive power compensation scheme for power distribution systems with generation from renewable sources has been proposed to improve the current quality of the distribution system. The proposed SAPF control scheme advantages are related to its simplicity, implementation and modeling. The use of a predictive control algorithm for the converter current loop proved to be an effective solution for improving current quality of the distribution system. The system tracking capability and transient response is improved. The predictive current controller is a stable and robust solution. The proposed algorithm mitigates the system harmonic currents and reactive power compensation simulated results have been shows the compensation effectiveness of the proposed active power filter.

## References

- [1] J. Rocabert, A. Luna, F. Blaabjerg, and P. Rodriguez, "Control of power converters in AC microgrids," *IEEE Trans. Power Electron.*, vol. 27, no. 11, pp. 4734–4749, Nov. 2012
- [2] M. Aredes, J. Hafner, and K. Heumann, "Three-phase four-wire shunt active filter control strategies," *IEEE Trans. Power Electron.*, vol. 12, no. 2, pp. 311–318, Mar. 1997
- [3] S. Naidu and D. Fernandes, "Dynamic voltage restorer based on a four leg voltage source converter," *Gener. Transm. Distrib., IET*, vol. 3, no. 5, pp. 437–447, May 2009
- [4] N. Prabhakar and M. Mishra, "Dynamic hysteresis current control to minimize switching for three-phase four-leg VSI topology to compensate nonlinear load," *IEEE Trans. Power Electron.*, vol. 25, no. 8, pp. 1935–1942, Aug. 2010.
- [5] V. Khadkikar, A. Chandra, and B. Singh, "Digital signal processor implementation and performance evaluation of split capacitor, four-leg and three h-bridge-based three-phase four-wire shunt active filters," *Power Electron., IET*, vol. 4, no. 4, pp. 463–470, Apr. 2011
- [6] F. Wang, J. Duarte, and M. Hendrix, "Grid-interfacing converter systems with enhanced voltage quality for microgrid application; concept and implementation," *IEEE Trans. Power Electron.*, vol. 26, no. 12, pp. 3501–3513, Dec. 2011.
- [7] X. Wei, "Study on digital pi control of current loop in active power filter," in *Proc. 2010 Int. Conf. Electr. Control Eng.*, Jun. 2010, pp. 4287–4290.
- [8] R. de Araujo Ribeiro, C. de Azevedo, and R. de Sousa, "A robust adaptive control strategy of active power filters for power-factor correction, harmonic compensation, and balancing of nonlinear loads," *IEEE Trans. Power Electron.*, vol. 27, no. 2, pp. 718–730, Feb. 2012.
- [9] J. Rodriguez, J. Pontt, C. Silva, P. Correa, P. Lezana, P. Cortes, and U. Ammann, "Predictive current control of a voltage source inverter," *IEEE Trans. Ind. Electron.*, vol. 54, no. 1, pp. 495–503, Feb. 2007.
- [10] P. Cortes, G. Ortiz, J. Yuz, J. Rodriguez, S. Vazquez, and L. Franquelo, "Model predictive control of an inverter with output LC filter for UPS applications," *IEEE Trans. Ind. Electron.*, vol. 56, no. 6, pp. 1875–1883, Jun. 2009.
- [11] R. Vargas, P. Cortes, U. Ammann, J. Rodriguez, and J. Pontt, "Predictive control of a three-phase neutral-point-clamped inverter," *IEEE Trans. Ind. Electron.*, vol. 54, no. 5, pp. 2697–2705, Oct. 2007.
- [12] P. Cortes, A. Wilson, S. Kouro, J. Rodriguez, and H. Abu-Rub, "Model predictive control of multilevel cascaded H-bridge inverters," *IEEE Trans. Ind. Electron.*, vol. 57, no. 8, pp. 2691–2699, Aug. 2010.
- [13] P. Lezana, R. Aguilera, and D. Quevedo, "Model predictive control of an asymmetric flying capacitor converter," *IEEE Trans. Ind. Electron.*, vol. 56, no. 6, pp. 1839–1846, Jun. 2009.
- [14] P. Correa, J. Rodriguez, I. Lizama, and D. Andler, "A predictive control scheme for current-source rectifiers," *IEEE Trans. Ind. Electron.*, vol. 56, no. 5, pp. 1813–1815, May 2009.
- [15] M. Rivera, J. Rodriguez, B. Wu, J. Espinoza, and C. Rojas, "Current control for an indirect matrix converter with filter resonance mitigation," *IEEE Trans. Ind. Electron.*, vol. 59, no. 1, pp. 71–79, Jan

## Author Profiles



**T. S. S. Mounisha** pursuing final year BTech in Sree Venkateswara College of Engineering



**M. V. Sushma** pursuing final year BTech in Sree Venkateswara College of engineering



**M. Neeraja** pursuing final year BTech in Sree Venkateswara College of engineering



**A. Venkatesh** pursuing final year BTech in Sree Venkateswara College of engineering



**E. Rambabu** obtained his BTech Degree in electrical and Electronics engineering. He Obtained MTech in JNTUA, Anthapuram